Supplementary material

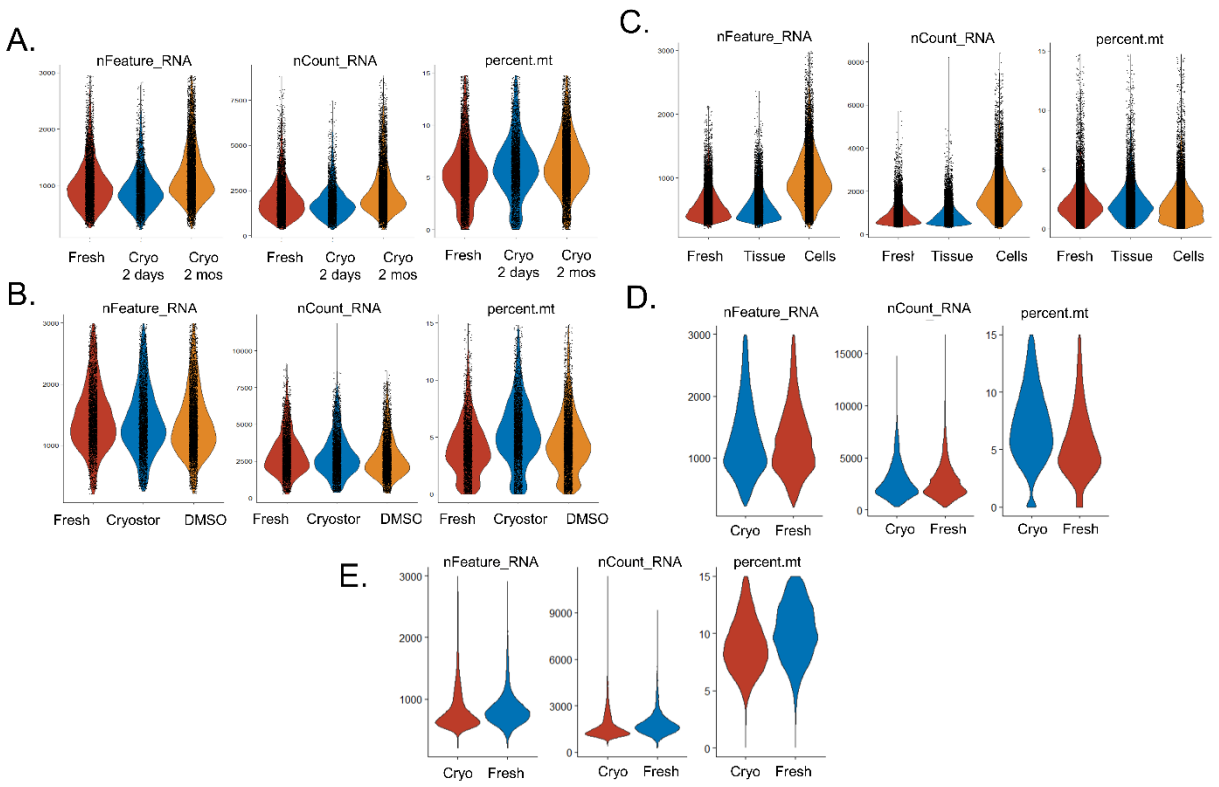

Supplementary Figure 1. Different cryopreservation strategies show no difference in single-cell RNA sequencing quality metrics. Violin plots show the number of genes in each cell (nFeature_RNA), the number of molecules in each cell (nCount_RNA), and the mitochondrial content for each cell (percent.mt). **(A)** Comparison of samples processed fresh, after cryopreservation for two days, or after cryopreservation for two months. **(B)** Comparison of samples processed fresh, after cryopreservation with a commercial DMSO-containing cryopreservative reagent (Cryostor), or after cryopreservation with 10% DMSO in fetal bovine serum. **(C)** Comparison of samples processed fresh, after whole-tissue cryopreservation, or after cryopreservation of enzymatically digested cells. **(D)** Comparison of three LNs processed fresh or cryopreserved, then sorted for $CD45^{-}EpCAM^{-}$ cells for scRNAseq. **(E)** Comparison of one LN processed fresh vs. cryopreserved for 18 months, followed by $CD45^{+}$ cell sorting for scRNAseq.

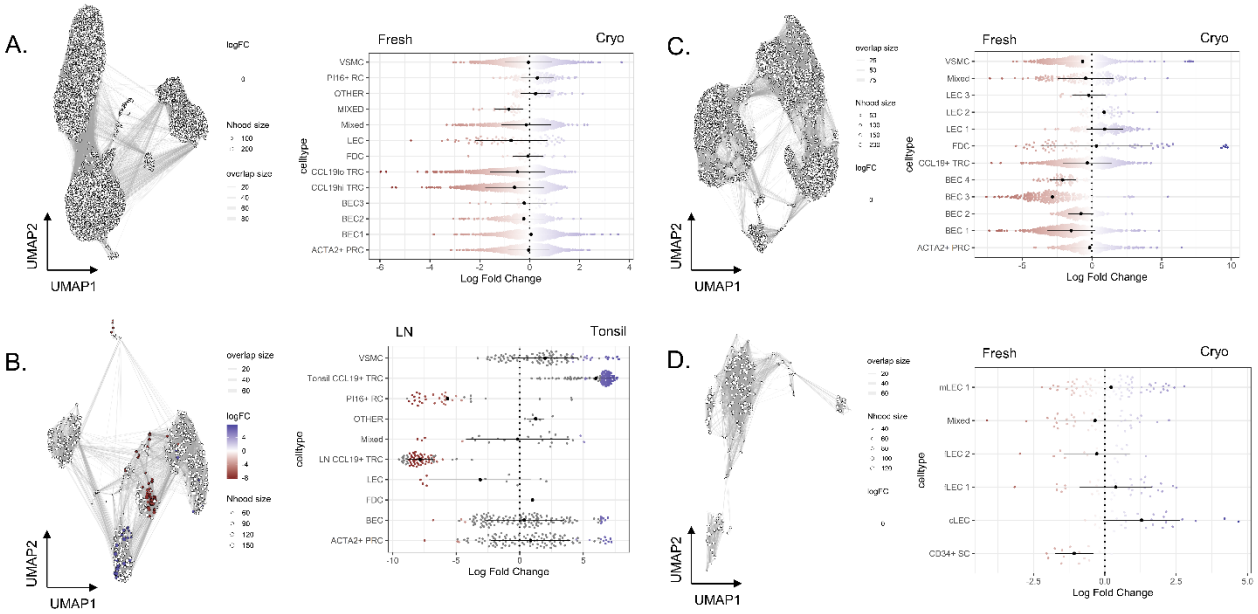

Supplementary Figure 2. Tonsillar stromal composition is unaffected by cryopreservation but varies from LN stroma. (A) *Left.* Milo neighborhoods superimposed on UMAP of CD45$^-$ EpCAM$^-$ cells from Figure 2 where dot size correlates with the number of cells in each neighborhood and line width correlates with overlap between neighborhoods. All neighborhoods are gray, indicating no differentially abundant (spatialFDR < 0.1) neighborhoods between fresh and cryopreserved tissue. *Right.* Bee-swarm plot of log-fold change (x-axis) across fresh and cryopreserved samples in Milo neighborhoods grouped together by Seurat-defined cell identity. Neighborhoods with ≥ 70% overlap with Seurat cell identity were included. Since all neighborhoods were not differentially abundant (spatialFDR > 0.99), all are shown on this plot (alpha = 1.0) with red indicating neighborhoods enriched in freshly processed tissue and blue indicating neihborhoods enriched in cryopreserved tissue. **(B)** *Left.* Milo neighborhoods superimposed on UMAP of tonsillar and LN cells from Supplementary Figure 5B where dot size correlates with the number of cells in each neighborhood and line width correlates with overlap between neighborhoods. Red indicates neighborhoods differentially abundant (spatialFDR < 0.1) in LNs and blue neighborhoods differentially abundant in tonsil between fresh and cryopreserved tissue. *Right.* Bee-swarm plot of log-fold change (x-axis) across fresh and cryopreserved samples in Milo neighborhoods grouped together by Seurat-defined cell identity. Only neighborhoods that were differentially abundant (spatialFDR < 0.1) are shown with significantly ($p < 0.05$) differentially abundant neighborhoods colored in red (for differentially abundant in LN) or blue (for differentially abundant in tonsil). **(C)** *Left.* Milo neighborhoods superimposed on UMAP of CD45$^-$EpCAM$^-$ cells from three LNs where dot size correlates with the number of cells in each neighborhood and line width correlates with overlap between neighborhoods. All neighborhoods are gray, indicating no differentially abundant (spatialFDR < 0.1) neighborhoods between fresh and cryopreserved tissue. *Right.* Bee-swarm plot of log-fold change (x-axis) across fresh and cryopreserved LNs in Milo neighborhoods grouped together by Seurat-defined cell identity. Since all neighborhoods were not differentially abundant (spatialFDR > 0.99), all are shown on this plot (alpha = 1.0) with red indicating neighborhoods enriched in freshly processed tissue and blue indicating neihborhoods enriched in cryopreserved tissue. **(D)** *Left.* Milo neighborhoods superimposed on UMAP of re-clustered

LECs from LNs where dot size correlates to number of cells in each neighborhood and line width correlates to overlap between neighborhoods. All neighborhoods are gray, indicating no differentially abundant (spatialFDR < 0.1) neighborhoods between fresh and cryopreserved tissue. *Right.* Bee-swarm plot of log-fold change (x-axis) across fresh and cryopreserved LNs in Milo neighborhoods grouped together by Seurat-defined cell identity. Since all neighborhoods were not differentially abundant (spatialFDR > 0.99), all are shown on this plot (alpha = 1.0) with red indicating neighborhoods enriched in freshly processed tissue and blue indicating neihborhoods enriched in cryopreserved tissue.

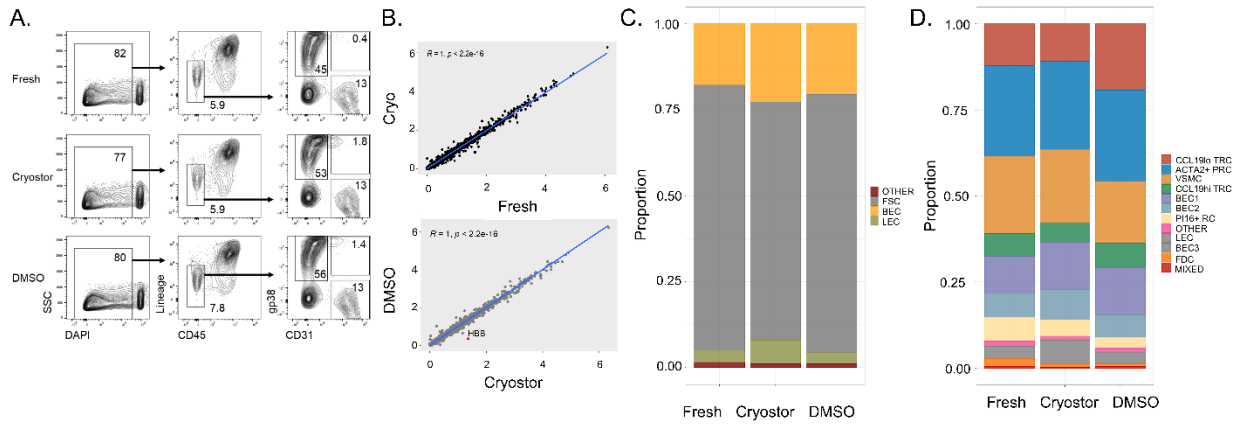

Supplementary Figure 3. Whole tissue cryopreservation is feasible with different DMSO-containing reagents. Tonsil pieces were either kept fresh in FBS-containing RPMI at 4°C for two days or cryopreserved for two days with a commercial DMSO-containing reagent (Cryostor) or 10% DMSO in fetal bovine serum. **(A)** Flow cytometric analysis of freshly processed tonsil and tonsil tissue cryopreserved with Cryostor or 10% DMSO in fetal bovine serum. The first column represents live/dead discrimination by DAPI uptake on all singlets. Live cells were then analyzed for expression of CD45 and hematopoetic lineage markers (CD3, CD14, CD16, CD19, CD20, CD56) in the second column with gating showing non-hematopoietic cells. These non-hematopoietic cells were then analyzed for expression of the fibroblast marker podoplanin (PDPN) and endothelial marker CD31 with gating showing fibroblastic stromal cells ($PDPN^{+}CD31^{-}$), blood endothelial cells ($PDPN^{-}CD31^{+}$), and lymphatic endothelial cells ($PDPN^{+}CD31^{+}$). **(B)** Linear regression of gene expression between (top) freshly processed and cryopreserved tonsil (with “cryo” referring to both Cryostor- and DMSO/FBS-preserved tissue). Linear regression of gene expression between (bottom) Cryostor- and DMSO/FBS-preserved tissue is also shown. Pearson correlation with associated p-value listed in graph with increased mRNA abundance in Cryostor-preserved tissue highlighted in red. **(C)** Colors in each bar define the proportions of each subset within the entire sample with fibroblastic stromal cells (FSCs) highlighted in grey, blood endothelial cells (BECs) in yellow, lymphatic endothelial cells (LECs) in green, and otherwise un-identified cells (other) in red. **(D)** Colors in each bar define proportions of each Seurat-defined cluster within the entire sample. Cluster identities were determined by expression of known markers as shown in Figure 2.

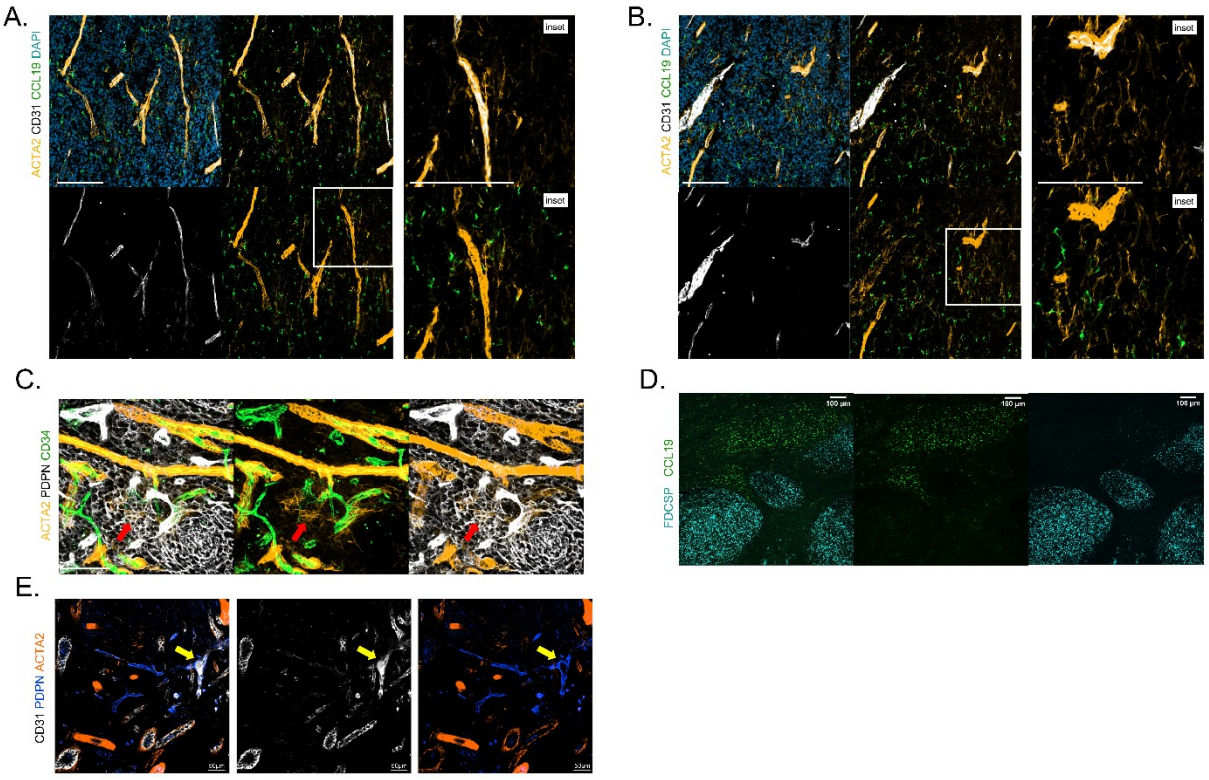

Supplementary Figure 4. Histologic appearance of lymphoid stromal cell subsets identified by single-cell RNA sequencing. (A) Immunofluorescent microscopy with 20X objective with staining for perivascular stromal cells by aSMA/ACTA2 (yellow), endothelial cells by CD31 (white), fibroblastic reticular cells by CCL19 (green), as well as DAPI for nuclear staining (blue). **(B)** Immunofluorescent microscopy with 20X objective of the tonsil interfollicular region with the same approach. **(C)** High-resolution imaging with 40X objective showing VSMC bright for ACTA2 staining (yellow) encircling endothelial cells expressing CD34 (green) with separate population of fibroblastic reticular cells identified via PDPN expression (white). Another population of ACTA2^{+} PRCs that dimly co-stain for ACTA2 and PDPN can also be identified (red arrow). **(D)** In situ hybridization with 25X objective of a tonsil showing germinal centers expressing the follicular dendritic cell marker FDCSP (blue) and interfollicular areas where cells express CCL19 (green). **(E)** Immunofluorescent microscopy with 20X objective shows ACTA2 (orange), PDPN (blue), and CD31 (white) with lymphatic endothelial cells noted to co-express PDPN and CD31 (yellow arrow).

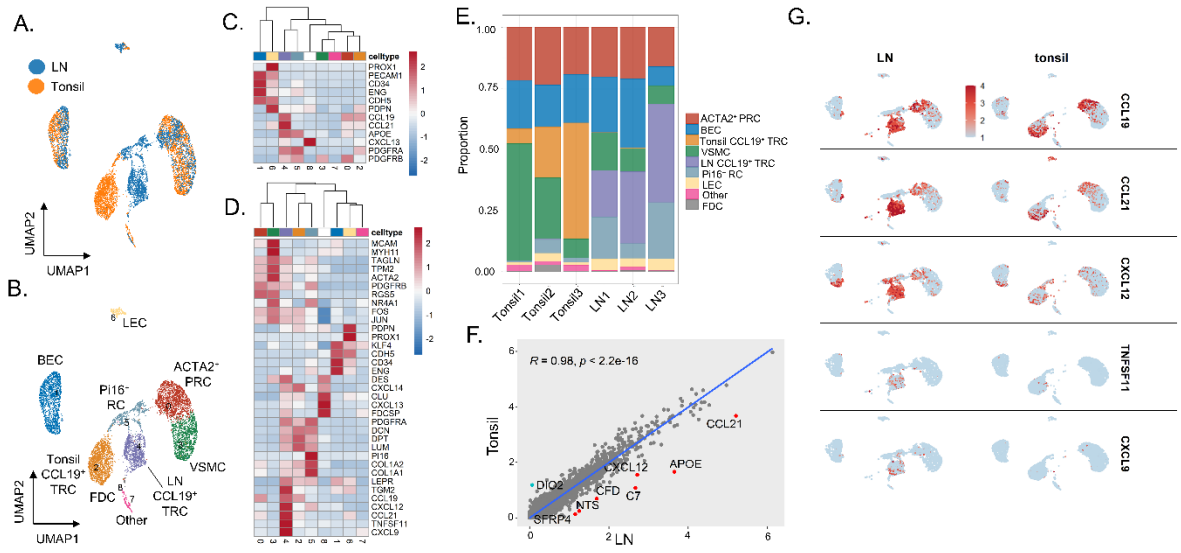

Supplementary Figure 5. Overlapping tonsillar and LN stromal cell subsets with more inflammatory immune-interacting CCL19⁺ TRC observed in LNs. Three freshly processed hyperplastic tonsils were compared to three LNs with reactive histologies following the schematic in Figure 1A. **(A)** UMAP shows all cells through Seurat-based clustering of sorted CD45⁻EpCAM⁻ cells after filters for quality control and removal of residual hematopoietic and epithelial cells with coloring based on lymphoid tissue type. **(B)** UMAP shows all cells through Seurat-defined clusters with labels based on subset identity derived from relative abundance of known marker gene mRNA. **(C)** Heatmap showing gene expression for Seurat-defined clusters of known markers for fibroblastic stromal cells (*PDGFRA, PDGFRB*, *CXCL13*, *APOE*, *CCL21*, *CCL19*, and *PDPN*), blood endothelial cells (*CDH5*, *ENG*, *CD34*, *PECAM1*), and lymphatic endothelial cells (*PROX1*, *PECAM1*, *PDPN*). **(D)** Heatmap showing gene expression of known markers for fibroblastic stromal cell subsets, including *ACTA2*⁺ perivascular reticular cells (*ACTA2*, *TAGLN*, *TPM2*, *PDGFRB*), vascular smooth muscle cells (*ACTA2*, *MYH11*, *MCAM*), CCL19^{hi} T-zone fibroblastic reticular cells (*CCL19*, *CCL21*, *CXCL12*, *CXCL9*), CCL19^{lo} T-zone fibroblastic reticular cells (*LUM*, *DCN*, *PDPN*, *PDGFRA*), Pi16⁺ reticular cells (*PI16*, *LEPR*), and follicular dendritic cells (*CXCL13*, *CLU*, *FDCSP*, *DES*). **(E)** Bar graph with colors in each bar defining proportions of each Seurat cluster. **(F)** Linear regression of gene expression between tonsils and LNs. Pearson correlation with associated p-value listed for genes showing up-regulated expression in LN tissue (highlighted in red) vs. down-regulated expression (highlighted in blue). **(G)** Feature plots showing relative expression of *CCL19*, *CCL21*, *CXCL12*, *TNFSF11*, and *CXCL9* in LN-derived and tonsil-derived samples.

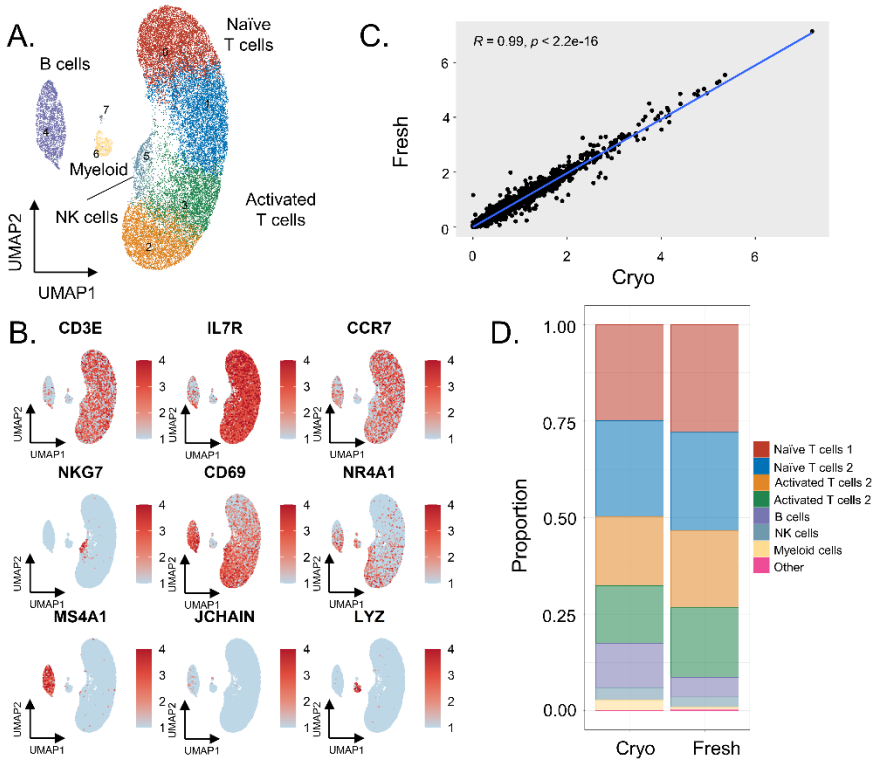

Supplementary Figure 6. Hematopoietic cells can be recovered after whole-tissue cryopreservation. An enlarged LN with an atypical T cell expansion was processed fresh on the day after surgical resection vs. cryopreserved for 18 months. The fresh or thawed cryopreserved tissue were enzymatically digested and sorted for CD45^{+} cells before scRNAseq. **(A)** UMAP shows all cells colored by Seurat-based clustering of sorted CD45^{+} cells after filters for quality control and removal of residual epithelial cells with labels based on subset identity derived from relative expression of known marker genes. **(B)** Feature plots showing relative expression of cluster-defining markers. **(C)** Linear regression of gene expression between the fresh and cryopreserved LN tissue. Pearson correlation with associated p-value. **(D)** Colors in each bar define proportions of each Seurat-defined cluster within the entire sample.

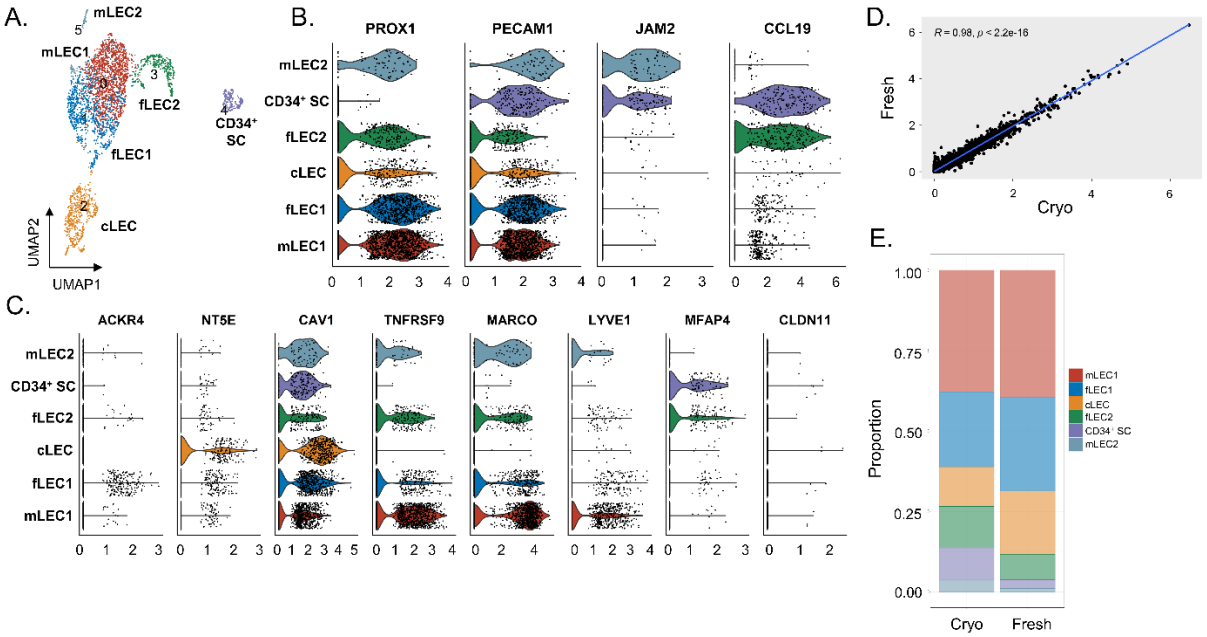

Supplementary Figure 7. Lymphatic endothelial cell subsets can be recovered and identified after whole-tissue cryopreservation. Re-clustering using only LECs from the three LNs that were processed fresh or after cryopreservation as described in Figure 5. **(A)** UMAP showing Seurat-based clustering with labeled cell-types based on expression of known markers. **(B)** Violin plots showing expression levels of LEC gene (*PROX1*), endothelial genes (*PECAM1, JAM2*), and fibroblast gene (*CCL19*) for each Seurat-defined cluster. **(C)** Violin plots showing expression of ceiling LEC (cLEC) genes (*NT5E*), medullary LEC (mLEC) genes (*CAV1*, *TNFRSF9*, *MARCO*), and floor LEC (fLEC) genes (*TNFRSF9*, *MFAP4*). **(D)** Linear regression of gene expression between the fresh and cryopreserved LN tissue. Pearson correlation with associated p-value. **(E)** Colors in each bar define proportions of each Seurat-defined cluster within the entire sample.